

# Food Mechanics: a New Device for Testing Fruits and Vegetables

**Antonio F. Ávila**

Senior Member, ABCM  
 aavila@netuno.lcc.ufmg.br  
 Universidade Federal de Minas Gerais  
 Department of Mechanical Engineering  
 31270-901 Belo Horizonte, MG, Brazil

**Gilva A. R. de Jesus**

gilva@demecc.ufmg.br

**Afzal A. Mesania**

afmesania@yahoo.com

**Alexandre S. Scari**

engscari@yahoo.com.br

The new mechanical device developed is capable of performing compression tests but also bending, torsion and tensile tests. Its measurement system has the following components: a load cell (0 to 9800 N), a strain gauge signal conditioning board, a plug-in general purpose data acquisition board, and a displacement sensor (0 to 29.7 mm). These components are connected to a personal computer that has specially developed software. The load cell consists of four extensometers, which are sensible to compressive load. The signal conditioning board filters and amplifies the signal, which is acquired by the AD converter, making this information available to be processed by the software. The device is powered by a DC motor (12 to 24 Volts). By setting the motor voltage, it is possible to control its rotation. The displacement sensor was made with a sliding potentiometer, which is pushed by the mobile component of the device while the tests are performed. Finally, the software provides the stress-strain diagram for each test. In order to guarantee reliable results, tests are made with cylindrical samples with same dimensions (radius and length). For the first set of tests, potatoes were studied. The test results for compressive showed an average value of 897.64 kPa. This value seems to be compatible to the ones from the literature. The device proves to be reliable. Moreover, its flexibility allowed testing a variety of fruits and vegetables under compression, tension, torsion and combined loads.  
**Keywords:** mechanical design, tensile and deformation measurements, mechanical device, fruits and vegetables mechanical properties, cellular materials testing

## Introduction

Thirty percent of all food produced in Brazil is lost by inadequate storage and transport conditions. In order to reduce these losses, it is crucial to design more efficient containers that can be stronger and offer more effective heat transfer conditions. The problem is that there is no database for tropical fruits and vegetables. The food mechanical properties data available are based on fruits and vegetables produced in the USA and in Europe.

In order to obtain this database, a new mechanical device was developed. From this point the new device will be called Food Testing Device (FTD). This equipment has to be sensible to a wide range of values so that it can capture the response of the large variety of tropical fruits and vegetable available in Brazil. Moreover, the grips have to be designed in such manner that an equilibrated tensile distribution at the contact region food/grip must be imposed. According to Fahloul et al (1996), the device must be reliable and with enough stiffness not to allow any interference from residual strains. In addition, the methodology used must follow pre-determined standards. One method that satisfies these criteria is the American Society for Testing of Materials (ASTM) standard test method for compressive properties of rigid plastics (ASTM, 1996). The compressive test supplies not only the compressive stress-strain diagram, but it also allows the user to identify the material fracture mode. A series of important information can be inferred from the stress-strain diagram, e.g. the compressive yield point, the modulus of elasticity and the percent compressive strain at the fracture.

Although the food mechanics seem to be simple, its design and analysis is not an easy task. The reason is that the large majority of fruits and vegetables are cellular materials. In addition, the network developed at microstructure level, as described by Gibson and Ashby (1997), and Laza et al. (2001) affect food mechanical properties. This means that the humidity inside the specimen has to be taken into consideration in the tests.

In many countries including Brazil the use of universal testing machines is widely spread for materials characterization. The use of these machines for testing fruits and vegetables can lead to a high increase on their price, as most of fixtures are not standard. The

prices for these "additions" can easily double the machine price. In fact, considering the average price of a universal testing machine and the cost for special fixtures, a testing machine for fruits and vegetables can easily exceed the one hundred thousand dollars value.

## Design and Device Capabilities

The device should be able to apply not only forces and moments, but also to measure the displacements and reaction forces during the tests. Forces and moments applied are quasi-static, i.e. they are applied in an incremental form in a speed close to 0.001 m/s. The device has three main parts. The first one is a DC electric motor with low speed and high torque. The second part is a speed reduction device. A roller chain composes this device and it is used for force multiplication from the electric motor to the main shaft. The last part is a power screw, where the torque is transformed into axial force. Figure 1 shows the device parts and identification.

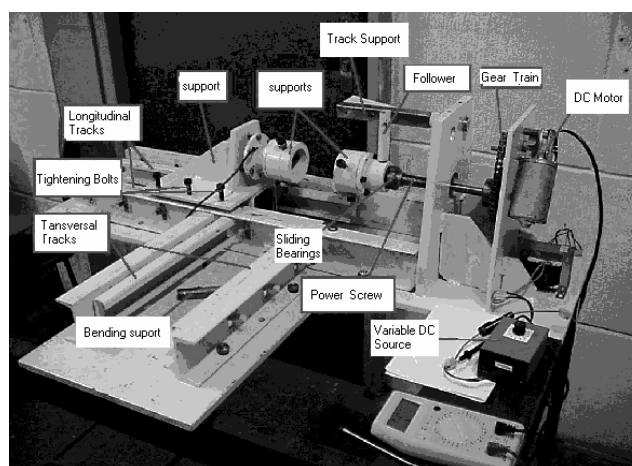


Figure 1. FTD Parts and Identification.

The DC electric motor has a maximum torque of 7 N.m at a 45 RPM, while the power screw has a trapezoidal shape, a nominal

diameter of 10 mm and a 1 mm lead. The roller chain speed ratio is 1:3, which leads to a 1 N.m maximum torque on the power screw.

The measurement system developed has the following components: a load cell, a strain gauge signal conditioning board, a plug-in general-purpose data acquisition board capable of measuring voltage signals (A/D converter), a personal computer and a specially developed software (Ozkul, 1996). The load cell, made of stainless steel 4340, is designed for force range from 0 to 9.78 KN. It has four strain gages, KFG-10-10-C1-11, connected by a full-bridge configuration, as shown in Figure 2. This configuration provides not only a greater sensitivity, but it also reduces the temperature influence on measurements. The strain gages supplied by Kyowa Corporation have gage length of 10 mm, gage resistance at 24°C and humidity of 50% of 10.0 ± 0.1 Ω, and a gage factor of 111 ± 0.1%.

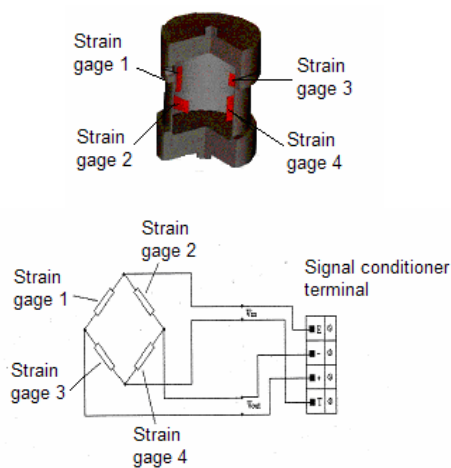


Figure 2. Load cell scheme.

The signal conditioner used provides options for full, half and one-fourth bridge connection. The A/D converter is connected to the computer's main board and it has a 16-bit resolution. The relationship between the voltage collected by the A/D converter and the force measured by the load cell is acquired by a calibration curve obtained by a two step procedure. The first step is a data base formation from the data acquired by the incremental forces measured by the load cell. The second step is a linear curve fitting. The procedure is repeated six times, and the mean values are used to construct the calibration curve. Figure 3 shows the calibration curve where voltage axis is pre-multiplied by a factor of 600. Notice that the R-square statistical parameter is close to unity. According to Montgomery (2001), this is an indication of a good curve fitting.

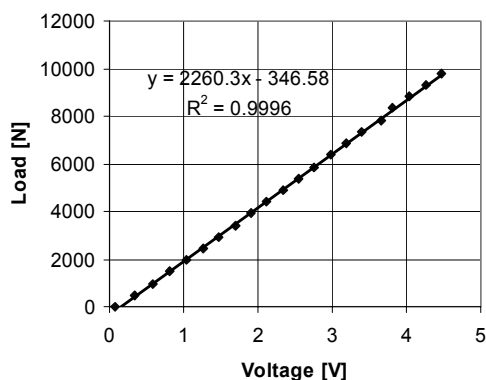


Figure 3. Calibration curve.

To collect the signals on real time, a data acquisition system is used. Figure 4 describes the main steps performed by the data acquisition code developed using LabVIEW®. The user must supply the following parameters: channel identification number where the load cell is connected, and the DC motor speed profile. The DC motor speed profile can be defined by a rising linear straight line or a piece-wise non-linear curve.

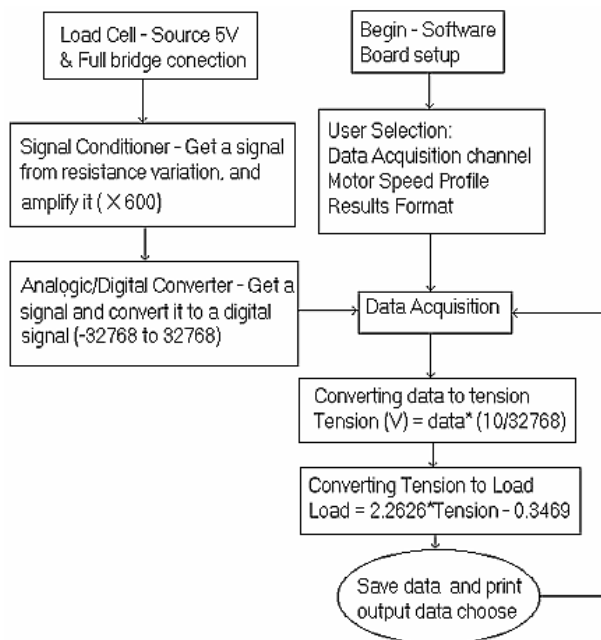


Figure 4. Data acquisition algorithm.

### Machine Certification

To demonstrate the FTD capabilities a set of experiments were performed. For the first set of experiments, the device stiffness was evaluated. It was considered an ANSI 1010 steel cylindrical specimen with half-inch (12.7 mm) diameter and ten inches (254.0 mm) length to carry out this analysis. The ratio diameter/length was such that buckling could be prevented. Compression, tension and torsion tests were executed, and displacements and/or strains on parts 1 through 5 were estimated. The part identification numbers are shown in Figure 5. Parts 1 through 5 are considered as critical regions since they are related to the machine fixtures where the specimens are positioned. Any non-considered displacement on the FTD design could impose a mismatch on specimen centerline and cause a specimen premature fracture. When possible, from each of the critical parts, the measurements of thickness variation and/or displacements were performed on the highest stress concentration region. As the force was gradually applied to the cylindrical specimen, the strains at each critical section were estimated by the following equation:

$$\epsilon = \frac{\Delta d}{d_0} \quad \text{or} \quad \epsilon = \frac{\Delta u}{u_0} \tag{1}$$

where,  $\epsilon$  is the strain on the direction of smallest cross section,  $\Delta d$  and  $\Delta u$  are diameter and displacement variation, respectively. The subscript  $o$  indicates the initial condition.

Taking into consideration the pre-test results, it was possible to conclude that there was no significant strain, less than 0.005 mm/mm, was developed in any of the five critical sections.

Therefore, the FTD stiffness was considered suitable, since the forces imposed on the steel specimens were close to the FTD ultimate load.

Notice that, although the device is capable of applying loads close to 50 KN, for safety reasons, the maximum operational loading was kept around 10 KN. This fact reinforces the device stiffness configuration.

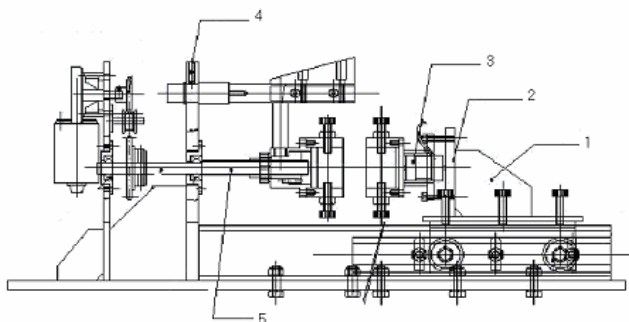


Figure 5. FTD critical parts.

Since the machine grips are made of nylon, the samples were attached by friction, as seen in Fig 6. The minimum and the maximum extension rate are  $13.47 \text{ m min}^{-1}$  ( $5 \square 1 \square \text{rpm}$ ) and  $37 \text{ m min}^{-1}$  ( $117.77 \text{ rpm}$ ), respectively. The device allows increase of the extension rate by setting the motor voltage. The extension rate used was the machine lower bound. During the compressive test, force and the displacement of the mobile grip were measured until the compressive yield point occurred in the samples. The software changed this database into tension and deformation providing the compressive stress-strain diagram.

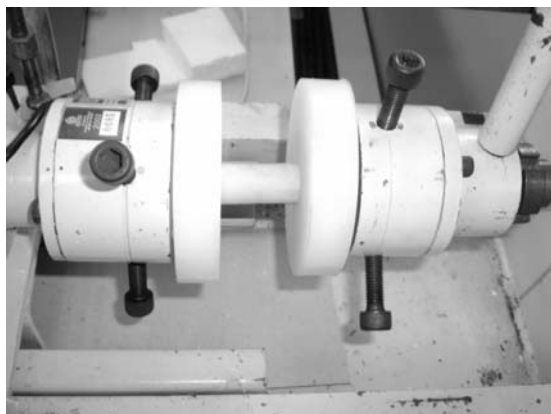


Figure 6. FTD grips for cylindrical specimens.

### Experimental Procedure

Two fruits and two vegetables were selected to check the FTD capabilities. As most of damages on fruits and vegetables are caused by compressive loadings, the compression test was the one performed during the experiments. The two vegetables were potato and yucca, while the fruits were pear and apple. The choice for yucca and potato was based on their high levels of consumption in Brazil, while pear and apples were selected due to their market high value. According to Horton (1987), the per capita consumption of potato in Brazil in 1983 was around  $1 \square \text{Kg}$ . Furthermore; there has been an increase in the consumption of potatoes not only in Brazil but also in many other countries. All fruits and vegetables were

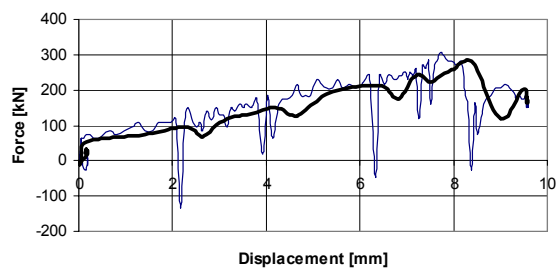
purchased in a local store, just before the test. The samples were prepared few minutes before the tests and all of them had a cylindrical shape.

Three sets of tests were made. In the first set of experiments only potatoes were studied. The samples length was kept constant and equal to 10 mm while two diameters were used, i.e. 11.0 mm or  $1 \square 8 \text{ mm}$ . The second group of experiments tested potatoes and pears. The samples' dimensions were: length – 40.0 mm (potato) and  $3.6 \text{ mm}$  (pear), diameter –  $0.7 \text{ mm}$  (potato) and 18.9 mm (pear). The last set of experiments focused on yucca and apple. For apple, the dimensions were: 18.3 mm in diameter and  $9 \text{ mm}$  in length, while for yucca, the diameter was  $0.4 \text{ mm}$ . Notice that due to brittle behavior of this vegetable length could not be fixed. As it is known longer lengths imply higher loadings, which can induce cracks inside the specimens.

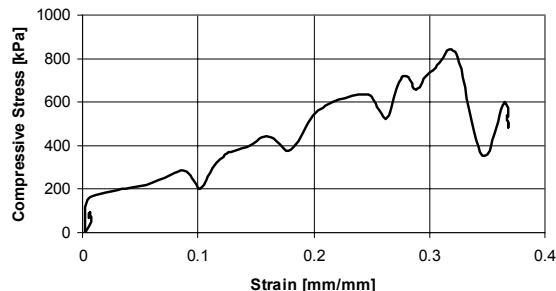
With a cylindrical tool, the samples were prepared minutes before the tests. This procedure was adopted to avoid loss of humidity. The number of samples tested was: 1  $\square$  potato samples for the first set of tests; 7 potato samples and  $\square$  pear samples for the second one and 5 apple samples and 6 yucca samples for the third set of tests.

### Experimental data: Analysis and discussion

The typical force-displacement curves without and with filter are shown in Fig. 7A, while the stress-strain curve can be seen in Fig. 7B. The filter could eliminate most of the noise captured during the tests of each potato set. For this case, the compressive yield point was set as the maximum value that the curve could reach. The sudden decrease at the end of the curve indicates that the sample fractured. By examining Fig 8, it is possible to conclude that fracture for most of potato specimens were caused by shear, as the fracture direction is on 45 degrees direction. The arrows indicate either complete or partial failure. The same methodology proposed by Green and Zerna (1968) for computing the elastic modulus can be applied here. In other words, the modulus of elasticity is the tangent of the angle between the straight line at the beginning of the curve and the x-axis.



a) Force-displacement chart



b) Stress-strain curve

Figure 7. Typical curves for potatoes.

To study the potato behavior under storage conditions, a series of five specimens were aligned, piled up and tested. The results are summarized in Table 1. The errors are 6.00 % for samples with 11.00 mm in diameter and 11.38 % for the ones with 11.80 mm in diameter. Potato, during the tests, suffered oxidation. According to Stroshine (1997), the oxidation can lead to changes on the mechanical as well as on physical-chemical properties of foods. Notice that there was no significant difference between single and aligned specimen's results. This is an indication that the piled up effect is not a major issue in this case.

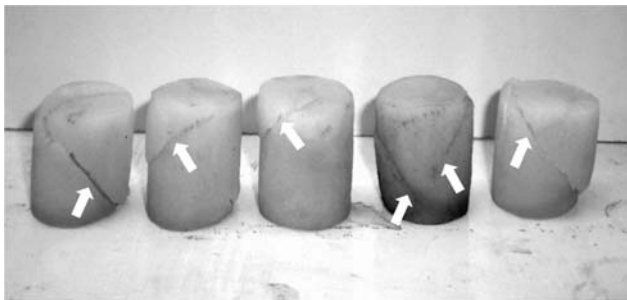


Figure 8. Shear failures into potato's samples.

Table 1. First set of results – Potatoes.

Sample	Diameter (mm)	Length (mm)	Compressive Stress (kPa)
single	11.00	10.00	103.31
aligned	11.00	10.00	970.34
single	11.80	10.00	110.19 ± 53.78
aligned	11.80	10.00	117.74 ± 10.78

To investigate the volume effect on mechanical properties, a new set of specimens were prepared. According to Thybo et al (2000), the specimen length is also a variable that can influence mechanical properties. The mean values for this set of experiments are listed in Table 2.

Table 2. Second set of results – Potatoes.

Group ID	Diameter [mm]	Length [mm]	Stress [kPa]	Strain [mm/mm]
1	11.00	6.00	1049.0	0.317
2	11.00	6.00	845.0	0.373
3	11.00	6.00	903.4	0.317
4	11.00	6.00	845.0	0.404
5	11.00	40.00	34.0	0.315
6	11.00	40.00	38.0	0.315

The potato samples humidity percentage was compatible to Thybo's results, see Fig. 9. Moreover, as expected, increases on length results lead to higher stresses. In fact, the average stress for the 6 mm length specimens' group was 897.64 ± 88.39 kPa, while for the 40 mm length samples the value was 1049.15 ± 83.38 kPa. The result confirm the hypothesis presented by Thybo et al. (2000), but is it possible to extrapolate this behavior to another vegetable?

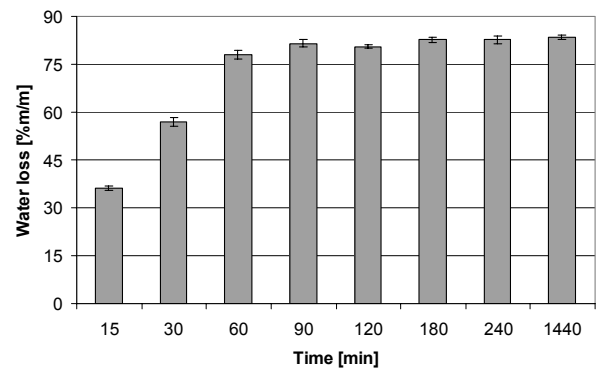


Figure 9. Water losses as a function of time – Potatoes.

To answer this question, sets of yucca samples were prepared. Due to its slipping conditions, the first sample was discarded. Table 3 summarizes the results. During sample preparation, it was observed that longer lengths were more difficult to obtain. As the length increases, cracks are generated during the cutting process leading to a premature failure.

Table 3. Third set of results – Yuccas.

Group ID	Diameter [mm]	Length [mm]	Stress [kPa]	Strain [mm/mm]
1	11.00	75	53.96	0.334
2	11.00	130	171.00	0.554
3	11.00	40	181.14	0.41
4	11.00	55	161.14	1.16
5	11.00	50	334.07	0.397

By analyzing Table 3, it is possible to conclude that the yucca behavior did not follow any behavior. This random performance can be explained by the natural anisotropy of this vegetable. Irish (2000) mentioned that yucca's morphology is highly dependent of climate conditions, soil nutrients, etc. Another important issue that can explain this random behavior is the presence of fibers. Considering the anisotropy of yucca and the presence of fibers, it is possible to draw an analogy between yucca and fibrous composites. As mentioned by Daniel and Ishai (1994), the increase on loadings guides to fiber micro buckling, and this leads to the formation of kink zones with excessive deformation. Figure 10 shows a stress-strain curve for yucca.

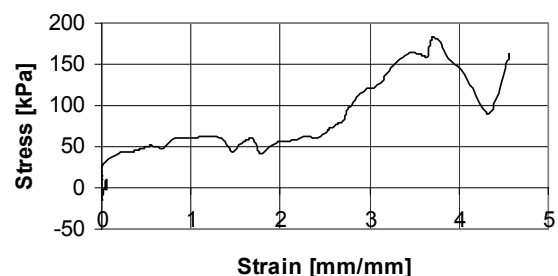


Figure 10. Typical stress-strain curve – Yucca.

The next set of experiments focused on fruits. The idea was to investigate how juicy fruits behave under compression. Note that those fruits have high market values and they are discarded if any damage is detected. Therefore, the design of more efficient containers is crucial. To improve the containers' design it is important to know the fruit mechanical behavior.

The first step is to identify the water loss rate as a function of time. It is important to determine the amount of humidity present during the compression tests. Figure 11 shows the rate of water loss for the apple samples. The result is compatible to the ones presented by Teskey and Shoemaker (1978).

As both, apples and pears, presents homogeneous microstructure, they were considered as quasi-isotropic materials. As a consequence the samples' diameter (18.90 mm) and length (19.90 mm) were fixed. Five apple samples were tested and the results are summarized in Table 4. Even though the samples were prepared same day, the results were highly influenced by the amount of juice present in each sample.

A typical apple stress-strain curve is shown in Fig. 12. At first, there was a high deformation (close to 0.3) that gradually decreased on stress with correspondent reduction on strain. After this initial stage, a gradual increase on stress implied correspondent increase on strain. This strange behavior can be attributed to the amount of water present inside the apple. An initial compression tends to induce water flow inside the sample, affecting its mechanical properties. In other words, the juice is "expelled" from the sample. Once the juice is expelled the "dry" apple behaves as a quasi-isotropic material. This behavior is described by Fig. 12. The final failure is clear on shear mode.

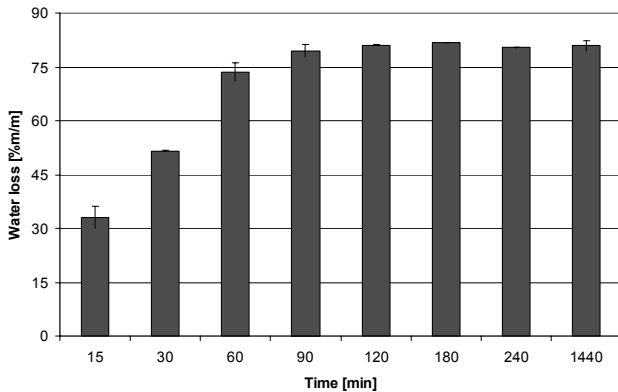


Figure 11. Water loss as a function of time – Apples.

Table 4. Fourth set of results – Apples.

Group ID	Diameter [mm]	Length [mm]	Stress [kPa]	Strain [mm/mm]
1	18.90	19.90	160.75	0.170
2	18.90	19.90	147.98	0.455
3	18.90	19.90	131.15	0.311
4	18.90	19.90	179.18	0.111
5	18.90	19.90	163.31	0.173

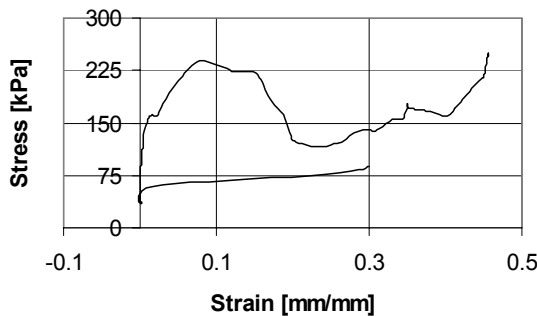


Figure 12. Typical stress-strain curve for apple.

For the pear samples a very strange behavior was observed. The juice formation was significant. This phenomenon can be noticed in Fig.13, the arrows show juice drops on fixtures. As a consequence of the large amount of juice coming out, the water flow inside the pear makes the sample behavior random and it is practically impossible to obtain reliable results. Even though the results seem to be "weird" some, hypothesis can be drawn from Fig 14, the stress-strain curve. The first hypothesis is that the induced water flow inside the pear seems to create an internal tensile field even though the external force applied is compressive. The second hypothesis is that this juice is randomly distributed inside the pear, and it is expelled at different times. The fracture, however, is a typical case of shear mode failure in a 45 degrees angle, as it can be observed in Fig. 15. Finally, a coupling between shear-tension is the most probable reason for this behavior. As mentioned by Jones (1999), the shear-tension coupling can be interpreted as the following: "a coupling is noticed when a tension is applied or induced and the failure is in shear mode."

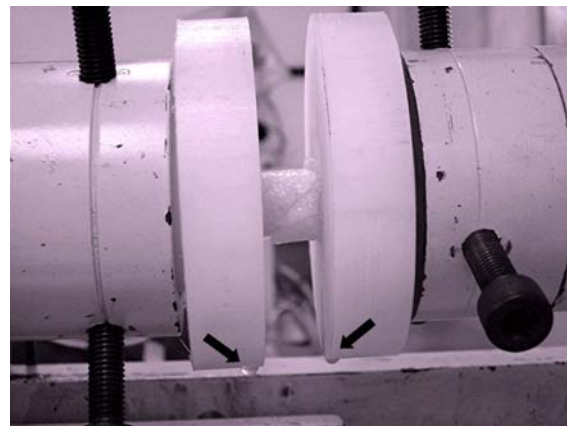


Figure 13. Juice coming out sample.

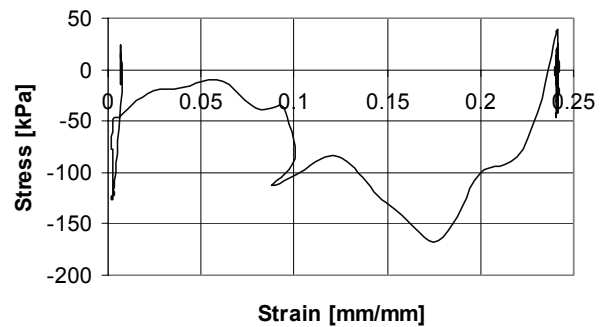


Figure 14. Typical stress-strain for pear.

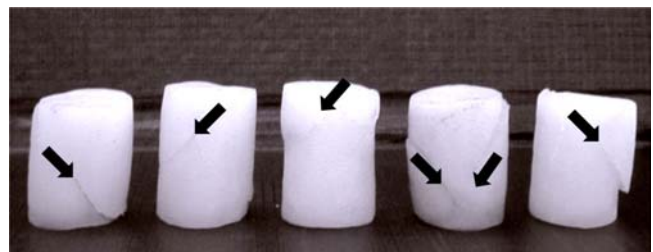


Figure 15. Shear mode failure into pear samples.

## Conclusions

The new device proves to be a helpful tool for studying food mechanical properties. The tests pointed to some patterns of behavior. First, the ultimate strength measured for the potatoes was around 1000 kPa. This result is compatible to the ones presented by Thybo et al. (2000). In addition, as discussed, the piled up effect does not affect the potato overall mechanical behavior. Since potatoes are homogeneous materials, their behavior is similar to other isotropic cellular materials. Second, when yucca was tested, a completely different performance was observed. The existence of fibers inside the yucca leads to a non-homogeneous stress distribution. The micro buckling mechanism of fibers was dominant during the compressive tests. This fact associated to the random distribution of fibers can explain the yucca's behavior. Last but not least, an investigation on juice fruits (apples and pears) was also performed. When under compression, the presence of water inside the fruits created an induce flow that affected their mechanical properties. This phenomenon was more evident when pears were studied. In this case, it seems that a tensile field inside the pear is induced even though the external loading is compressive. This phenomenon can be explained by shear-tension coupling caused by the pear's natural anisotropy and by the juice induced flow.

## Acknowledgments

The authors would like to acknowledge the financial support and grants provided by the Universidade Federal de Minas Gerais.

## References

- ASTM D 695-96, 1996, "Standard Test Method for Compressive Properties of Rigid Plastics", Annual Book of American Society for Testing Materials, pp. 77-83.
- Daniel, I.M., Ishai, O., 1994 "Engineering Mechanics of Composite Materials", Oxford UP, Oxford, UK, 395p.
- Fahloul D., Scalon M. G., Dushnicky L. G. and Symons S. J., 1996, "The Fracture Toughness of Pea Test in Relation to Temperature Abuse During Frozen Storage", Food Research International, Vol. 19, No. 8, pp. 791-797.
- Gibson, L. J., Ashby, M., 1997, "Cellular Solids: Structures and Properties", Cambridge University Press, 2<sup>nd</sup> edition, New York, pp. 93-174.
- Green, A.E., Zerna, W., 1968, "Theoretical Elasticity", Dover Publications Inc. New York, 457p.
- Horton, D.E., 1987 "Potatoes: Production, Marketing, and Programs for Developing Countries", Westview Press, Boulder, USA, 403p.
- Irish, M., 2000 "Agaves, Yuccas, and Related Plants: A Gardener's Guide", Timber Press, Portland, USA, 177p.
- Jones, R.M., 1999, "Mechanics of Composite Materials", Taylor and Francis, New York, USA, 311p.
- Laza, M., Scanlon, M. G., Mazza, G., 2001, "The effect of tuber pre-heating temperature and storage time on the mechanical properties of potatoes", Food Research International, Vol. 34, pp.659-667.
- Montgomery, D.C., 2001 "Design and Analysis of Experiments", John Wiley Publishers, New York, USA, 430p.
- Ozkul, T., 1996, "Data Acquisition and Process Control using Personal Computers", Marcell Dekker Publishers, New York, 157p.
- Stroshine, Richard, 1997, "Physical Properties of Agricultural Material and Food Products", West Lafayette, Purdue University Press, 107p.
- Teskey, B.J.E., Shoemaker, J.S., 1978 "Tree Fruit Production", Avi Pulishers, Westport, USA, 157p.
- Thybo, A. K., Bechmann, I. E., Martens M. and Engelsen, S. B., 2000, "Prediction of Sensory Texture of Cooked Potatoes using Uniaxial Compression, Near Infrared Spectroscopy and Low Field 1H NMR Spectroscopy", Lebensmittel-Wissenschaft und-Technologie, Vol. 33, pp. 103-111.